Occlusion-Aware Video Registration for Highly Non-Rigid Objects Supplementary Material

Bertram Taetz*[1,2], Gabriele Bleser†[1,2], Vladislav Golyanik‡[1], and Didier Stricker§[1,2]

[1]German Research Center for Artificial Intelligence, Kaiserslautern, Germany
[2]Department of Computer Science, Technical University Kaiserslautern, Kaiserslautern, Germany

Abstract

To give additional insight into our proposed method we present the optimization methods that we used to minimize the proposed energies of the occlsion-aware multi-frame optical flow (MFOF) as well as the global denoising of the occlusion probability maps. Furthermore, we added further examples, including dense NRSfM reconstructions, to demonstrate the capabilities of the proposed method.

1. Introduction

We first describe the minimization methods that are used to minimize the energies of the proposed occlusion-aware MFOF method. In order to obtain a MFOF method that is highly accurate and well parallelizable we cast the energy minimizations into the framework of the efficient primal dual method of [3]. Thereafter further examples follow.

2. Used primal dual algorithms

This section gives details about the different primal dual algorithms used for the minimization tasks of the proposed approach. These minimization algorithms are similar to different parts of [5], [1] and [7]. In the following we often use algorithms of [3] that are applicable to saddle-point problems of the from

$$\min_{x\in X}\max_{y\in Y}\langle Kx, y\rangle - F^*(y) + G(x). \tag{1}$$

This is a primal-dual formulation of the nonlinear minimization problem

$$\min_{x\in X} F(Kx) + G(x). \tag{2}$$

*Bertram.Taetz@dfki.de
†Bleser@cs.uni-kl.de
‡Vladislav.Golyanik@dfki.de
§Didier.Stricker@dfki.de

Here we assume the following: X, Y be finite-dimensional real vector spaces with an inner product $\langle\cdot,\cdot\rangle$. The map $K : X \to Y$ is a continuous linear operator, $G : X \to [0,\infty)$, and $F^* : Y \to [0,\infty)$, being proper, convex, lower semi-continuous with F^* being the convex conjugate of a convex lower semicontinuous function F.
The original form of the MFOF [5] is

$$E[\mathbf{u}(\mathbf{x},n),\mathbf{L}(\mathbf{x})] = \alpha E_{\text{data}} + \beta E_{\text{link}} + E_{\text{reg}}, \tag{3}$$

with

$$E_{\text{data}} = \int_\Omega \sum_{n=1}^{F} \Phi(\mathbf{I}(\mathbf{x}+\mathbf{u}(\mathbf{x},n),n) - \mathbf{I}(\mathbf{x},n_0))\,d\mathbf{x} \tag{4}$$

$$E_{\text{link}} = \int_\Omega \sum_{n=1}^{F} |\mathbf{u}(\mathbf{x},n) - \sum_{i=1}^{R} \mathbf{q}_i(n) L_i(\mathbf{x})|^2\,d\mathbf{x} \tag{5}$$

$$E_{\text{reg}} = \int_\Omega \sum_{r=1}^{R} g(\mathbf{x})\Phi(\nabla L_r(\mathbf{x}))\,d\mathbf{x}. \tag{6}$$

We now focus on the minimization of the modified form

$$E_{\xi(\mathbf{x},n)}[\mathbf{u}(\mathbf{x},n),\mathbf{L}(\mathbf{x})] = (1-\xi(\mathbf{x},n))[\alpha E_{\text{data}}] + \beta E_{\text{link}} + E_{\text{reg}}, \tag{7}$$

with

$$\mathbf{u}(\mathbf{x},n) = \begin{cases} \sum_{i=1}^{R} \mathbf{q}_i(n) L_i(\mathbf{x}) & \text{if} \quad \xi(\mathbf{x},n) = 1 \\ \mathbf{u}(\mathbf{x},n) & \text{if} \quad \xi(\mathbf{x},n) = 0 \end{cases}. \tag{8}$$

2.1. Primal dual algorithm of proposed MFOF for minimization with respect to $\mathbf{u}$

In this section we describe the minimization method for the energy of the occlusion aware MFOF, namely $E_{\xi(\mathbf{x},n)}[\mathbf{u}(\mathbf{x},n),\mathbf{L}(\mathbf{x})]$ with respect to $\mathbf{u}(\mathbf{x},n)$, given the occlusion maps $\xi(\mathbf{x},n)$.

Thus, we keep $\mathbf{L}(\mathbf{x})$ fixed and observe that E_{data} and E_{link} depend on $\mathbf{u}(\mathbf{x}, n)$ and therefore we need to minimize

$$(1-\xi(\mathbf{x},n))[\alpha E_{\text{data}}] + \beta E_{\text{link}} = \tag{9}$$
$$\alpha \int_\Omega \sum_{n=1}^{F} (1-\xi(\mathbf{x},n)\Phi(\mathbf{I}((\mathbf{x}+\mathbf{u}),n) - \mathbf{I}(\mathbf{x},n_0))\, d\mathbf{x}$$
$$+\beta \int_\Omega \sum_{n=1}^{F} \left| \mathbf{u}(\mathbf{x},n) - \sum_{i=1}^{R} \mathbf{q}_i(n) L_i(\mathbf{x}) \right|^2 d\mathbf{x}$$

with respect to $\mathbf{u}(\mathbf{x}, n)$. Note that due to the definition of $\mathbf{u}(\mathbf{x}, n)$ we have $(1 - \xi(\mathbf{x}, n))[\alpha E_{\text{data}}] + \beta E_{\text{link}} = (1 - \xi(\mathbf{x}, n))[\alpha E_{\text{data}} + \beta E_{\text{link}}]$. For this minimization step we modified the dual formulation of [5] as follows. We take the $L1$-norm $\Phi(v) = |v|$ and linearize the data term E_{data} around $\mathbf{x} + \mathbf{u}_0(\mathbf{x}, n)$. Moreover, we substitute $\mathbf{u}' = \sum_{i=1}^{R} \mathbf{q}_i(n) L_i(\mathbf{x})$, thus (9) can be rewritten as

$$E^{aux}(\mathbf{u}) = \alpha(1-\xi)|\mathbf{A}\mathbf{u} + \mathbf{b}| + \beta|\mathbf{u} - \mathbf{u}'|^2 \tag{10}$$

with $\mathbf{b} = \mathbf{I}(\mathbf{x} + \mathbf{u}_0, n) - \mathbf{I}(\mathbf{x}), n_0) - \mathbf{A}\mathbf{u}_0$ and $\mathbf{A} = \frac{\partial \mathbf{I}(\mathbf{x}+\mathbf{u}_0,n)}{\partial \mathbf{x}}$ being the $N_c \times 2$ Jacobian of the n-th frame, evaluated at $\mathbf{x} + \mathbf{u}_0$. We also introduced the short notation $\xi = \xi(\mathbf{x}, n)$. Therefore, we have to solve the minimization problem

$$\min_{\mathbf{u}} \alpha(1-\xi)|\mathbf{A}\mathbf{u} + \mathbf{b}| + \beta|\mathbf{u} - \mathbf{u}'|^2 \tag{11}$$

The convex conjugate (Legendre-Fenchel transform) of $\Phi(v) = |v|$ is $\Phi^*(v) = \delta(v)$ with

$$\delta(v) = \begin{cases} 0 & \text{if } |v| \le 1 \\ \infty & \text{if } |v| \ge 1 \end{cases}.$$

Moreover, $|v|$ is a proper convex and lower semi-continuous function. For dualization we intepret $F(\alpha(\mathbf{A}\mathbf{u} + b)) = |\alpha(\mathbf{A}\mathbf{u} + \mathbf{b})|$ leading to the convex conjugate $F^*(\mathcal{I}) = \delta(\mathcal{I}/\alpha) - \langle \mathbf{b}, \mathcal{I} \rangle$. Thus, the dualized energy, including the bi-conjugate and the coupling term, reads

$$E^{aux}(\mathbf{u}) =$$
$$(1-\xi) \max_{\mathcal{I}} \{ \langle \mathbf{A}\mathbf{u}, \mathcal{I} \rangle + \langle \mathbf{b}, \mathcal{I} \rangle - \delta\left(\frac{\mathcal{I}}{\alpha}\right) \}$$
$$+\beta|\mathbf{u} - \mathbf{u}'|^2. \tag{12}$$

We can now write the minimization (11) as saddle-point problem

$$\min_{\mathbf{u}} \max_{\mathcal{I}} \left\{ (1-\xi)[\langle \mathbf{A}\mathbf{u}, \mathcal{I} \rangle + \langle \mathbf{b}, \mathcal{I} \rangle] - \delta\left(\frac{\mathcal{I}}{\alpha}\right) + \beta|\mathbf{u} - \mathbf{u}'|^2 \right\}. \tag{13}$$

Taking $K = \mathbf{A}\mathbf{u}$ and realizing that the function $G(\mathbf{u}) = \beta|\mathbf{u} - \mathbf{u}'|^2$ is a convex function with convexity parameter 2β, we can cast (13) into the form (1) and are able to apply the primal dual algorithm 2 of [3]. We obtain the following iteration method for the optimization of (13) inside the alternation approach:

- Choose $\sigma_0 = \tau_0 = \frac{1}{L_A}$
- Initialize $\mathbf{u}_0$ and $\mathcal{I}$ from previous alternation iteration
- Initialize $\bar{\mathbf{u}}_0 = \mathbf{u}_0$
- Iterate for $k = 0, 1, 2, \ldots$ until a convergence criterion is satisfied

$$\mathcal{I}^{k+1} = \Gamma_\alpha \left(\mathcal{I}^k + \tau_k(1-\xi)(\mathbf{A}\bar{\mathbf{u}}^k + \mathbf{b}) \right)$$
$$\mathbf{u}^{k+1} = \tfrac{1}{1+2\sigma_k\beta} \left(2\sigma_k\beta\mathbf{u}' + \mathbf{u}^k - \sigma_k(1-\xi)\mathbf{A}^T\mathcal{I}^{k+1} \right)$$
$$\theta_k = \tfrac{1}{\sqrt{1+4\beta\sigma_k}},\ \sigma_{k+1} = \theta_k\sigma_k,\ \tau_{k+1} = \tfrac{\tau_k}{\theta_k}$$
$$\bar{\mathbf{u}}^{k+1} = \mathbf{u}^{k+1} + \theta_k(\mathbf{u}^{k+1} - \mathbf{u}^k).$$

Note that we initialize $\mathbf{u}^0 = 0$ and $\mathcal{I}^0 = 0$ at the beginning of the pyramid approach and prolongate the updated variables through the pyramids as described in [9]. Furthermore, we choose

$$L_A = \max_{n=1,\ldots,F} \Big(\max_{i,j \in \text{Img}} \Big(\underbrace{\max_{r=1,\ldots,N_c} \sum_{c=1}^{2} |a_{rc}|}_{\text{maxnorm of Jacobian } \mathbf{A}_{i,j}} \Big) \Big). \tag{14}$$

The projection Γ is here defined as:

$$\Gamma_\alpha(\mathbf{s}) = \frac{\mathbf{s}}{\max(1, \frac{|\mathbf{s}|}{\alpha})}.$$

We declare convergence, if the relative update $\frac{\mathbf{u}^{k+1} - \mathbf{u}^k}{\mathbf{u}^k}$ is negligible with respect to some threshold (e.g. 10^{-3}).

2.2. Primal dual algorithm of proposed MFOF for minimization with respect to $\mathbf{L}(\mathbf{x})$

In this section we describe the minimization method for the energy $E_{\xi(\mathbf{x},n)}[\mathbf{u}(\mathbf{x}, n), \mathbf{L}(\mathbf{x})]$ with respect to $\mathbf{L}(\mathbf{x})$, given $\xi(\mathbf{x}, n)$. We keep $\mathbf{u}(\mathbf{x}, n)$ fixed and observe that E_{link} and E_{reg} depend on $\mathbf{L}(\mathbf{x})$. Therefore we have to minimize

$$E_{\text{reg}} + \beta E_{\text{link}} = \tag{15}$$
$$\int_\Omega \sum_{n=1}^{F} \left| \mathbf{u}(\mathbf{x},n) - \sum_{i=1}^{R} \mathbf{q}_i(n) L_i(\mathbf{x}) \right|^2 d\mathbf{x} \tag{16}$$
$$+ \int_\Omega \sum_{i=1}^{R} g(\mathbf{x}) \Phi(\nabla L_i(\mathbf{x}))\, d\mathbf{x} \tag{17}$$

In contrast to the minimization above, we choose Φ to be the Huber-norm with parameter ϵ, i.e.

$$\Phi(v) = \Phi(v)_\epsilon = \begin{cases} \frac{|v|^2}{2} & \text{if} |v| \leq \epsilon \\ |v| - \frac{\epsilon}{2} & \text{if} |v| > \epsilon. \end{cases} \quad (18)$$

We decompose the vector of all displacements $[\mathbf{u}(\mathbf{x},1),\ldots,\mathbf{u}(\mathbf{x},F)]^T$ into two orthonormal parts. One is the projection of the displacements onto the trajectory subspace spanned by the basis trajectories $\mathbf{q}_i(n),\ldots,\mathbf{q}_R(n)$ and the other one is its orthogonal complement. Similar to [5] we can argue that the orthogonal complement is constant with respect to $\mathbf{L}(\mathbf{x})$ and can thus be left out of the minimization. Therefore it is equivalent to penalize deviations of $\mathbf{u}(\mathbf{x},n)$ to $\sum_{i=1}^R \mathbf{q}_i L_i(x)$, which lies on the subspace, or penalizing the distance of $\sum_{i=1}^R \mathbf{q}_i L_i(x)$ with respect to the projection of $\mathbf{u}(\mathbf{x},n)$ to the subspace. The coefficients $\mathbf{M}(\mathbf{x})$ define the projection onto the trajectory subspace and can be obtained from the trajectories and the displacements as follows

$$\mathbf{M}(\mathbf{x}) = \begin{pmatrix} [\sum_{n=1}^F \mathbf{q}^T \mathbf{u}(\mathbf{x},n)]_1 \\ \vdots \\ [\sum_{n=1}^F \mathbf{q}^T \mathbf{u}(\mathbf{x},n)]_R \end{pmatrix}. \quad (19)$$

The linking term E_{link} can thus be rewritten as

$$\int_\Omega \sum_{n=1}^F \left| \mathbf{u}(\mathbf{x},n) - \sum_{i=1}^R \mathbf{q}_i(n) L_i(\mathbf{x}) \right|^2 \quad (20)$$

$$= \int_\Omega \sum_{i=1}^R (M_i(x) - L_i(x))^2. \quad (21)$$

This leads to a decoupling of the coefficients $L(x)_i$ which allows us to optimize for each $L_i(x)$ separately. Subsequently, the minimization of (15) boils down to the minimization of

$$\sum_{i=1}^R \int_\Omega g(\mathbf{x}) |\nabla L_i(\mathbf{x})|_\epsilon + \beta (M_i(\mathbf{x})) - L_i(\mathbf{x}))^2 \, d\mathbf{x}, \quad (22)$$

which can be optimized separately for each $i = 1,\ldots,R$. Dropping the index i for simplicity, we are left with the minimization problem

$$\min_L \int_\Omega g(\mathbf{x}) |\nabla L(\mathbf{x})|_\epsilon + \beta (M(\mathbf{x})) - L(\mathbf{x}))^2 \, d\mathbf{x}. \quad (23)$$

In a similar manner as described before, we can obtain a saddle point problem that reads

$$\min_L \max_{\mathcal{L}} \left\{ \langle \nabla L(\mathbf{x}), \mathcal{L}(\mathbf{x}) \rangle - \delta \left(\frac{\mathcal{L}(\mathbf{x})}{g(\mathbf{x})} \right) - \epsilon \frac{|\mathcal{L}|^2}{2g(\mathbf{x})} \right.$$
$$\left. + \beta (M(\mathbf{x}) - L(\mathbf{x}))^2 \right\} \quad (24)$$

This fits in to the form (1) by taking $K = \nabla$, which is bounded by $\sqrt{8}$. $G(\mathbf{x}) = \beta(M(\mathbf{x}) - L(\mathbf{x}))^2$ with convexity parameter 2β and $F^* = \delta\left(\frac{\mathcal{L}(\mathbf{x})}{g(\mathbf{x})}\right) - \epsilon \frac{|\mathcal{L}|^2}{2g(\mathbf{x})}$ with convexity parameter ϵ. We can now use a variant of algorithm 3 proposed in [3] and obtain the following algorithm

- Initialize $L^0(\mathbf{x}) = \bar{L^0}(\mathbf{x}) = M(\mathbf{x})$, $\mathcal{L}^0$ from previous alternation iteration
- Iterate for $k = 0, 1, 2, \ldots$ until a convergence criterion is satisfied

$$\mathcal{L}^{k+1} = \Gamma_{g(\mathbf{x})} \left(\frac{\mathcal{L}^k + \tau \nabla \bar{L}^k(\mathbf{x})}{1 + \frac{\tau\epsilon}{g(\mathbf{x})}} \right)$$
$$L^{k+1} = \frac{1}{1+2\sigma\beta} \left(2\sigma\beta M(\mathbf{x}) + L^k(\mathbf{x}) + \sigma div(\mathcal{L}^{k+1}) \right)$$
$$\bar{L}^{k+1} = 2L^{k+1}(\mathbf{x}) - L^k(\mathbf{x}))$$

We initialize $L^0 = 0$ and $\mathcal{L}^0 = 0$ on the highest pyramid level and prologate the values as in [9]. Here $div(\cdot)$ is the divergence operator which is the negative dual operator to the gradient operator ∇. Both operators are discrete and implemented as detailed in [3]. The stepsizes are chosen to be

$$\sigma = \sqrt{\frac{\epsilon}{16\beta}}, \;\; \tau = \sqrt{\frac{\beta}{4\epsilon}}, \quad (25)$$

which guarantees convergence in the sense of [3].

2.3. Primal Dual Algorithm for occlusion map denoising

In this section we describe the minimization method for the energy $E_{\text{occl}}[\xi(\mathbf{x},n)]$ and thus the algorithm for **Step 3** in the proposed occlusion aware MFOF approach.
This energy can be optimized seperately from the energy (3), since it only denoises the pre-estimates $\tilde{\xi}(\mathbf{x},n)$ of the occlusion map. The methods proposed here are related to [1] and the general form of the problem is inspired by [7]. In the following we write down a general form of the algorithm that we used with the parameters $\gamma = 1$, $\epsilon_{\text{occl}} = 1$ and $W = \text{diag}(1,1,0.01)$ in our experiments. We minimize

$$\gamma E_{\text{occl}} = \quad (26)$$
$$\gamma \int_\Omega \sum_{n=1}^F (\xi(\mathbf{x},n) - \tilde{\xi}(\mathbf{x},n))^2 + \Phi(\nabla_3 \xi(\mathbf{x},n)) \, d\mathbf{x},$$

where Φ is the Huber-norm with parameter ϵ_{occl}. We define $\nabla_3 \xi(\mathbf{x},n) = W \nabla \xi(\mathbf{x},n)$ as weighted spatial-temporal gradient, with the diagonal matrix W as given above. In a similar way as before, we can derive a saddle-point problem for this energy

$$\min_\xi \max_\eta \left\{ \langle W \nabla \xi, \eta \rangle - \delta \left(\frac{\eta}{\gamma} \right) - \frac{\epsilon_{\text{occl}}}{2\gamma} \|\eta\|^2 \right. \quad (27)$$
$$\left. + \gamma (\xi - \tilde{\xi})^2 \right\} \quad (28)$$

We left out the explicit space and time dependencies $(\mathbf{x}, n)$ for reasons of better readability. This problem can be cast into the form of problem (1), by taking $K = \nabla$ and consequently $F^*(\eta) = \delta(\frac{\eta}{\gamma})$, as well as $G(\xi) = \gamma(\xi - \tilde{\xi})^2$ with convexity parameter 2γ. Therefore we can apply algorithm 3 of [3], which yields the following.
Initialize $\xi^0 = \xi_0$ (e.g. $\xi_0 = 0$, or a given initial occlusion map) and $\eta^0 = 0$ at the highest pyramid level. In each alternation iteration along the image space and image sequence (time) $(\mathbf{x}, n)$ do the following iteration

- Initialize $\xi^0 = \bar{\xi}^0$, η^0 from previous alternation iteration
- Iterate for $k = 0, 1, 2, \ldots$ until a convergence criterion is satisfied

$$\eta^{k+1} = \Gamma_\gamma \left(\frac{\eta^k + \tau \nabla \bar{\xi}^k}{1 + \frac{\tau \epsilon_{\text{occl}}}{\gamma}} \right)$$

$$\xi^{k+1} = \frac{1}{1+2\sigma\gamma} \left(\xi^k + \sigma(div(W\eta^{k+1}) + 2\gamma\tilde{\xi}) \right)$$

$$\bar{\xi}^{k+1} = 2\xi^{k+1} - \xi^k$$

$$\xi^{k+1} = \max(\min(\xi^{k+1}, 1), 0)$$

$$\bar{\xi}^{k+1} = \max(\min(\bar{\xi}^{k+1}, 1), 0).$$

Note that taking $\bar{\xi}^{k+1} = \xi^{k+1}$ gives slightly better convergence rates, but might have numberical stability issues in special cases, see [3]. By restricting the matrix entries of the diagonal matrix W to $0 \leq w_{i,j} \leq 1$ the discrete version of $\|div(W\eta)\|^2$ is bounded by $\sqrt{12}$. This can be shown in an analogous way as the bound of $\sqrt{8}$ for the discrete version of $\|div(W\eta)\|^2$ in the case $W = \text{diag}(1, 1, 0)$ as was previously proofed in [2]. Therefore, we use the step size $\sigma = \sqrt{\frac{\epsilon_{\text{occl}}}{24\gamma}}$ and $\tau = \sqrt{\frac{\gamma}{6\epsilon_{\text{occl}}}}$, which guarantees convergence as previously mentioned in the sense of [3].

3. Further tests on real data

3.1. Dense NRSfM of waving flag

In this section we show dense NRSfM reconstructions of the waving flag sequence with large occlusions, applied to the correspondences computed from the base scheme and the proposed method (MFOF Prop.-3).
We base the NRSfM reconstruction on [6] for the flag sequence with respect to frame 26, using the base scheme as well as the proposed scheme, textured with the reference frame. It is clearly visable that the reconstruction based on the corrected correspondences of the proposed scheme is less distored, in the occluded regions, than the reconstruction based on the base scheme. Note, that we used the non-occluded texture here to better visualize the effect of the wrong correspondences.

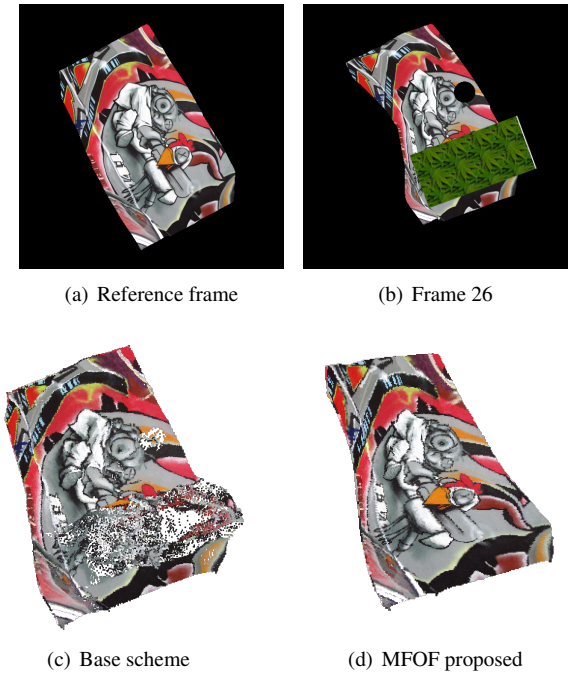

(a) Reference frame (b) Frame 26

(c) Base scheme (d) MFOF proposed

Figure 1: NRSfM reconstructions of the waving flag based on MFOF correspondences, from the base scheme (left) and the proposed method (right).

3.2. Turning head scenario

We also tested the proposed method on a sequence obtained from a consumer camera. It shows a turning head of a man. The sequence contains 38 RGB-images (480×470 pixels). Due to some low texture regions, we computed the optical flow based on the gradients of the color images (a 6 dimensional vector for each pixel), like in the heart sequence example (in the paper). In Figure 2 we illustrate the different components used for the occlusion probability estimation in this scenario. The reference frame and frame 32 of the sequence are shown in the top row. Below the operation of our algorithm is illustrated on the rather large occlusions caused by the turning head. Shown are the occlusion indicators as well as the initial and the denoised occlusion probability maps. It can be observed that the counter indicator (Figure 2(c)) captures mostly self-occlusions, while the divergence indicator (Figure 2(d)) captures both self-occlusions and newly incoming parts of the head. The result of the proposed Bayesian smoother shows already reasonably well defined local regions (Figure 2(e)), which are thereafter globally refined via variational denoising (Figure 2(f)). This test case demonstrates that the occlusion estimation framework can not only be used to improve the flow fields, as shown before, but also for providing a general visibility measure with respect to the given reference frame or template. This information can be useful, *e.g.* for auto-

(a) Reference image (b) 32th image

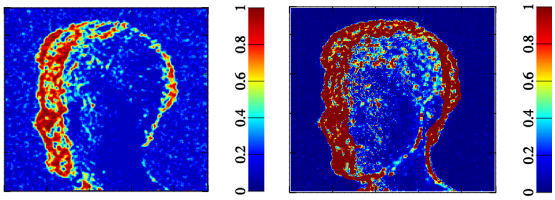

(c) Counter indicator (d) Divergence indicator

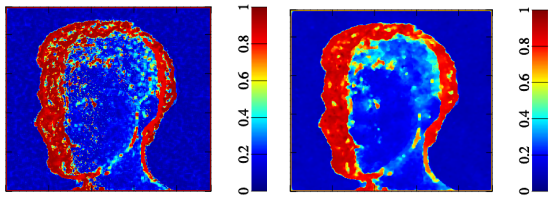

(e) Pre-estimate (f) Final probability map

(g) Final backwarp (occlusions marked black)

Figure 2: Illustration of our proposed method on a real-world sequence.

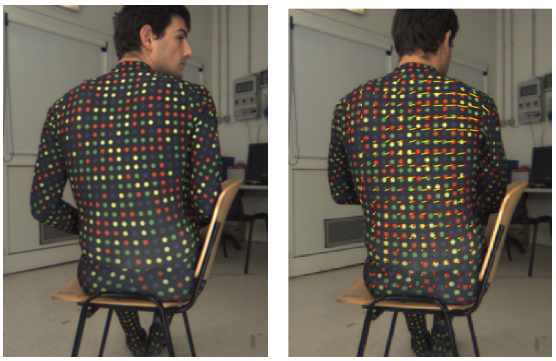

(a) Reference (b) Corr. 10

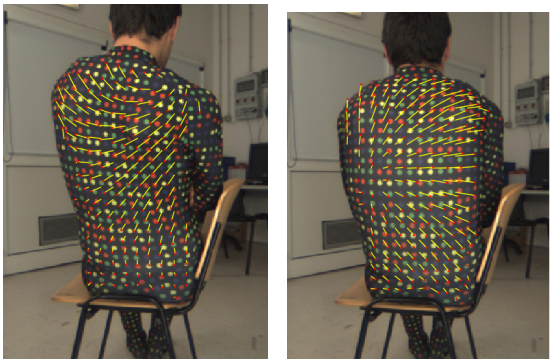

(c) Corr. 89 (d) Corr. 139

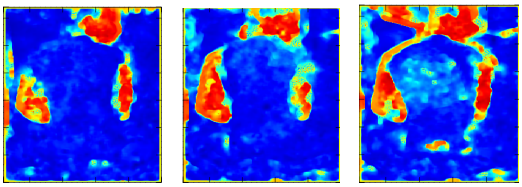

(e) Occl. prob. 10 (f) Occl. prob. 89 (g) Occl. prob. 139

(h) Frame 10 (i) Frame 89 (j) Frame 139

Figure 3: Correspondences, occlusion probabilities and some NRSfM reconstructions of the back sequence.

matic video segmentation as well as for automatic selection of new reference images in long video sequences. Note the good correspondences of the visible part of the head using the proposed MFOF method, as indicated by the backward warp shown in Figure 2(g). Here, regions with high probability of occlusion (> 0.5) have been colored black.

3.3. Deforming Back Sequence

The back sequence [8] is a 150 frame long sequence showing a person deforming sideways and stretching. This sequence has already been reconstructed with rather high precision using the correspondences of the base scheme together with the NRSfM method of [4]. We show results of our algorithm on this sequence, to demonstrate additional insight that can be gained through the flow uncertatinty map and to demonstrate that the quality of the final NRSfM reconstruction will not be harmed through the proposed approach. Figure 3 shows correspondences from frame 10, 89, 139 of the backsequence, with occlussion / flow uncertainty probabilities shown in 3(e), 3(f) and 3(g). These maps clearly indicate regions with uncertain flow estimates. This is useful information for correspondence selection, correction as well as video segmentation for NRSfM reconstructions.

We present NRSfM results based on the correspondences of the proposed method in 3, using again the method [4], to confirm the high quality reconstructions that can be obtained with the computed correspondences. Note that, although the person is moving and considerably deforming the back, our method works reliably and does not spuriously mark the parts of non-rigid deformations.

4. Conclusion

We presented the algorithms behind the variational optimization steps of the MFOF method and the denoising of the occlusion pre-estimate in space and time. Moreover, several additional examples demonstrate the methods potential in different scenarios.

References

[1] C. Ballester, L. Garrido, V. Lazcano, and V. Caselles. A tv-l1 optical flow method with occlusion detection. In A. Pinz, T. Pock, H. Bischof, and F. Leberl, editors, *DAGM/OAGM Symposium*, volume 7476 of *Lecture Notes in Computer Science*, pages 31–40. Springer, 2012.

[2] A. Chambolle. An algorithm for total variation minimization and applications. *J. Math. Imaging Vis.*, 20(1-2):89–97, Jan. 2004.

[3] A. Chambolle and T. Pock. A first-order primal-dual algorithm for convex problems with applications to imaging. *J. Math. Imaging Vis.*, 40(1):120–145, May 2011.

[4] R. Garg, A. Roussos, and L. Agapito. Dense variational reconstruction of non-rigid surfaces from monocular video. In *The IEEE Conference on Computer Vision and Pattern Recognition (CVPR)*, 2013.

[5] R. Garg, A. Roussos, and L. Agapito. A variational approach to video registration with subspace constraints. *International Journal of Computer Vision*, pages 1–29, 2013.

[6] M. Paladini, A. D. Bue, J. M. F. Xavier, L. de Agapito, M. Stosic, and M. Dodig. Optimal metric projections for deformable and articulated structure-from-motion. *International Journal of Computer Vision*, 96(2):252–276, 2012.

[7] S. Ricco and C. Tomasi. Dense lagrangian motion estimation with occlusions. In *CVPR*, pages 1800–1807. IEEE, 2012.

[8] C. Russell, J. Fayad, and L. Agapito. Energy based multiple model fitting for non-rigid structure from motion. In *Computer Vision and Pattern Recognition (CVPR), 2011 IEEE Conference on*, pages 3009–3016, June 2011.

[9] A. Wedel, T. Pock, C. Zach, H. Bischof, and D. Cremers. An improved algorithm for tv-l 1 optical flow. In D. Cremers, B. Rosenhahn, A. Yuille, and F. Schmidt, editors, *Statistical and Geometrical Approaches to Visual Motion Analysis*, volume 5604 of *Lecture Notes in Computer Science*, pages 23–45. Springer Berlin Heidelberg, 2009.